Journal of Circuits, Systems, and Computers
Vol. 12, No. 5 (2003) 563–591
© World Scientific Publishing Company

World Scientific
www.worldscientific.com

OPTIMIZATION OF FREQUENCY-RESPONSE MASKING BASED FIR FILTERS

TAPIO SARAMÄKI* and JUHA YLI-KAAKINEN†

Institute of Signal Processing, Tampere University of Technology,
P. O. Box 553, FIN-33101, Tampere, Finland
**saram@vip.fi*
**ts@cs.tut.fi*
†*ylikaaki@cs.tut.fi*

HÅKAN JOHANSSON

Division of Electronics Systems, Department of Electrical Engineering,
Linköping University, SE-58183 Linköping, Sweden
hakanj@isy.liu.se

A very efficient technique to drastically reduce the number of multipliers and adders in implementing linear-phase finite-impulse response (FIR) digital filters in applications demanding a narrow transition band is to use the frequency-response masking (FRM) approach originally introduced by Lim. The arithmetic complexity can be even further reduced using a common filter part for constructing the masking filters originally proposed by Lim and Lian. A drawback in the above-mentioned original FRM synthesis techniques is that the subfilters in the overall implementations are separately designed. In order to further reduce the arithmetic complexity in these two FRM approaches, the following two-step optimization technique is proposed for simultaneously optimizing the subfilters. At the first step, a good suboptimal solution is found by using a simple iterative algorithm. At the second step, this solution is then used as a start-up solution for further optimization being carried out by using an efficient unconstrained nonlinear optimization algorithm. An example taken from the literature illustrates that both the number of multipliers and the number of adders for the resulting optimized filter are less than 80% compared with those of the FRM filter obtained using the original FRM design schemes in the case where the masking filters are separately implemented. If a common filter part is used for realizing the masking filters, then an additional reduction of more than 10% is achieved compared with the optimized design with separately implemented masking filters.

Keywords: Frequency-response masking approach; narrow transition-band digital filters; FIR filters; optimization.

1. Introduction

One of the most efficient techniques for synthesizing narrow transition band linear-phase finite-impulse response (FIR) digital filters with a drastically reduced number of multipliers and adders compared with the conventional direct-form implementation is the frequency-response masking (FRM) approach.[1–4] The price to be paid

for this reduction in the arithmetic complexity is a slight increase in the overall filter order. The arithmetic complexity of FIR filters based on the use of the FRM approach can be even further reduced using a common filter part for constructing the masking filters.[5]

A drawback of the original FRM synthesis techniques [1–5] for both of the above-mentioned FIR filter classes is that the subfilters have been separately designed. This paper proposes a two-step technique for reducing the overall arithmetic complexity by simultaneously designing all the subfilters. Some parts of the material in this contribution has been presented earlier in the conference articles.[6,7] At the first step, in the case of separate masking filters, a simple iterative design scheme is used for generating a start-up solution for further optimization.[6] At the second step, this solution is then improved with the aid of an efficient unconstrained nonlinear optimization algorithm. An example taken from the literature shows that in the case of separate masking filters both the number of multipliers and the number of adders of the resulting optimized filter are less than 80% compared to those of the FRM filter obtained by using the original FRM design schemes described in Refs. 1–4.

In order to even further reduce the filter complexity, a similar simultaneous optimization scheme is applied for synthesizing filters where the masking filters are generated using a common filter part.[7] The motivation for considering these generalized filters lies in the fact that the magnitude responses for the masking filters after the simultaneous optimization are very similar (see, e.g., Fig. 6 in Ref. 6 or Fig. 8 in this contribution). The same example as for the case of separate masking filters shows that by properly using a common filter part for synthesizing the masking filters results in an additional reduction of more than 10% in the overall filter complexity.

This paper is organized as follows: Sec. 2 reviews the basic idea of using the FRM approach for generating computationally-efficient linear-phase FIR filters for applications demanding a narrow transition band as well as briefly describes the original synthesis schemes for their design. Section 3 concentrates on simultaneously optimizing all the subfilters in the case where the masking filters are separately implemented. It proposes a two-step technique where a start-up filter is first determined using a simple iterative algorithm and then improved with the aid of an efficient nonlinear unconstrained optimization algorithm. Section 4 shows how to estimate various filter design parameters in order to arrive at the optimized filter with the lowest number of multipliers and adders to meet the given criteria. A two-step design scheme similar to that used in Sec. 3 is applied in Sec. 5 for designing filters where the masking filters share a common filter part. Section 6 shows, by means of an example taken from the literature, that the filters optimized using the proposed techniques provide the above-mentioned benefits over the original FRM designs. Finally, concluding remarks are drawn in Sec. 7.

2. Frequency-Response Masking (FRM) Approach

This section reviews how to use the original FRM approach for synthesizing linear-phase FIR filters.

2.1. *Filter structure and frequency response*

In the FRM approach, the linear-phase FIR filter transfer function is constructed as follows:

$$H(z) = F(z^L)G_1(z) + \left[z^{-LN_F/2} - F(z^L)\right]G_2(z)\,, \tag{1a}$$

where

$$F(z^L) = \sum_{n=0}^{N_F} f(n)z^{-nL}\,, \tag{1b}$$

$$G_1(z) = z^{-M_1}\sum_{n=0}^{N_1} g_1(n)z^{-n}\,, \tag{1c}$$

and

$$G_2(z) = z^{-M_2}\sum_{n=0}^{N_2} g_2(n)z^{-n}\,. \tag{1d}$$

Here, the impulse-response coefficients $f(n)$, $g_1(n)$, and $g_2(n)$ possess an even symmetry. N_F is even, whereas both N_1 and N_2 are either even or odd. For $N_1 = N_2$, $M_1 = M_2 = 0$, whereas for $N_1 > N_2$ [$N_1 < N_2$], $M_1 = 0$ and $M_2 = (N_1 - N_2)/2$ [$M_1 = (N_2 - N_1)/2$ and $M_2 = 0$]. These selections guarantee that the delays of both of the terms of $H(z)$ are equal. An efficient implementation for the overall filter is depicted in Fig. 1, where the delay term $z^{-LN_F/2}$ is shared with $F(z^L)$. $G_1(z)$ and $G_2(z)$ can also share their delays if a transposed direct-form implementation (exploiting the coefficient symmetry) is used.

The zero-phase frequency response of $H(z)$ (the phase term $e^{-jM\omega/2}$ with $M = LN_F + \max\{N_1, N_2\}$ is omitted) can be expressed as

$$H(\omega) = H_1(\omega) + H_2(\omega)\,, \tag{2a}$$

where

$$H_1(\omega) = F(L\omega)G_1(\omega) \tag{2b}$$

and

$$H_2(\omega) = [1 - F(L\omega)]G_2(\omega) \tag{2c}$$

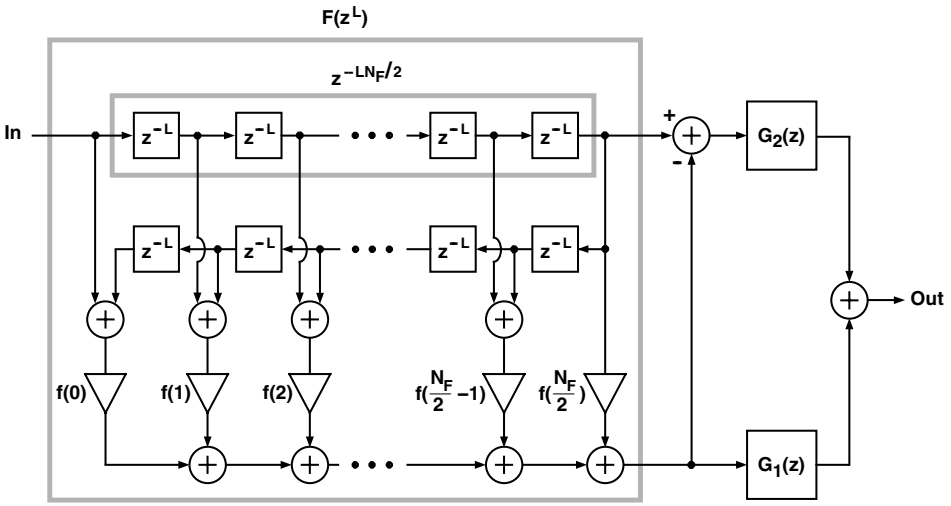

Fig. 1. An efficient implementation for a filter synthesized using the FRM approach.

with

$$F(\omega) = f\left(\frac{N_F}{2}\right) + 2\sum_{n=1}^{N_F/2} f\left(\frac{N_F}{2} - n\right)\cos n\omega \tag{2d}$$

and for $k = 1, 2$

$$G_k(\omega) = \begin{cases} g_k\left(\dfrac{N_k}{2}\right) + 2\displaystyle\sum_{n=1}^{N_k/2} g_k\left(\frac{N_k}{2} - n\right)\cos n\omega & \text{for } N_k \text{ even}\,, \\ \displaystyle\sum_{n=0}^{(N_k-1)/2} g_k\left(\frac{N_k - 1}{2} - n\right)\cos\left[\left(n + \frac{1}{2}\right)\omega\right] & \text{for } N_k \text{ odd}\,. \end{cases} \tag{2e}$$

2.2. *Efficiency of the use of the transfer function* $F(z^L)$

The efficiency of $H(z)$, as given by Eq. (1), lies in the fact that the pair of transfer functions $F(z^L)$ and $z^{-LN_F/2} - F(z^L)$ can be generated from the pair of *prototype* transfer functions $F(z) = \sum_{n=0}^{N_F} f(n)z^{-n}$ and $z^{-N_F/2} - F(z)$ by replacing z^{-1} by z^{-L}. This increases the filter orders to LN_F, but since only every Lth impulse-response value is nonzero, both the number of multipliers and the number of adders remain the same. The above prototype pair forms a *magnitude-complementary* filter pair since their zero-phase frequency responses, $F(\omega)$ and $1 - F(\omega)$ with $F(\omega)$ given by Eq. (2d), add up to unity. Figure 2(a) illustrates the relations between these responses in the case of a lowpass–highpass filter pair with passband and stopband edges being located at θ and ϕ.

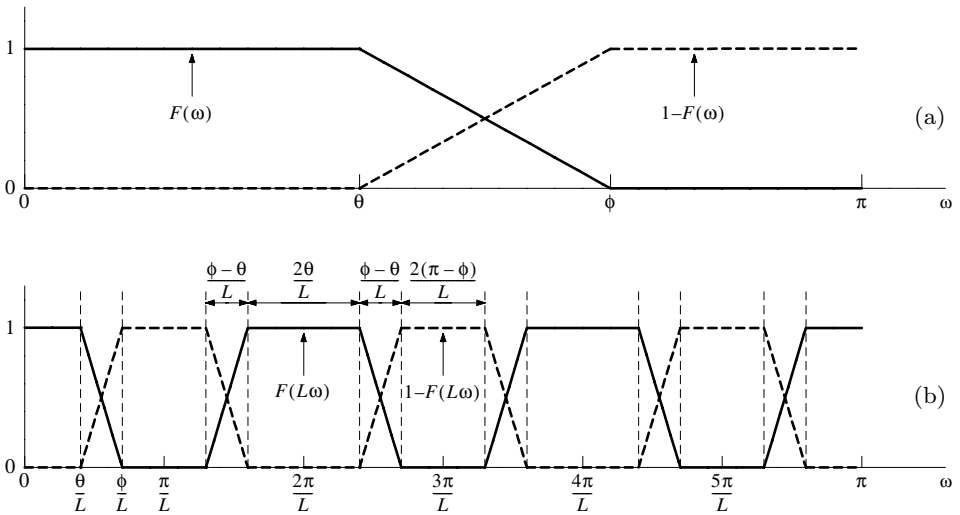

Fig. 2. Generation of a magnitude-complementary periodic filter pair by starting with a lowpass–highpass complementary pair. (a) Prototype filter responses $F(\omega)$ and $1 - F(\omega)$. (b) Periodic responses $F(L\omega)$ and $1 - F(L\omega)$ for $L = 6$.

As illustrated in Fig. 2(b), the substitution $z^{-L} \mapsto z^{-1}$ preserves the complementary property resulting in the *periodic*[a] responses $F(L\omega)$ and $1 - F(L\omega)$ that are frequency-axis compressed versions of the prototype responses such that the interval $[0,\ L\pi]$ is shrunk onto $[0,\ \pi]$. Since the period of the prototype responses is 2π, the period of the resulting responses is $2\pi/L$ and they contain several passband and stopband regions in the interval $[0,\ \pi]$.

For a lowpass overall transfer function $H(z)$, one of the transition bands provided by $F(z^L)$ or $z^{-LN_F/2} - F(z^L)$ can be used as that of the overall filter. In the first case, denoted by a Case A design, the passband and stopband edges are given by (see Fig. 3)

$$\omega_p = \frac{2l\pi + \theta}{L} \quad \text{and} \quad \omega_s = \frac{2l\pi + \phi}{L}\,, \tag{3}$$

respectively, where l is a fixed non-negative integer, and in the second case, referred to as a Case B design, by (see Fig. 4)[b]

$$\omega_p = \frac{2l\pi - \phi}{L} \quad \text{and} \quad \omega_s = \frac{2l\pi - \theta}{L}\,. \tag{4}$$

[a]Throughout this paper, the term "periodic" is used to emphasize the fact that the zero-phase frequency responses of both $F(z^L)$ and $z^{-LN_F/2} - F(z^L)$ contain several periods in the baseband region $[0,\ \pi]$.

[b]In practice, ω_p and ω_s are given and the remaining problem is to determine whether a Case A design or a Case B design gives the minimum arithmetic complexity. For this purpose, the design parameters L, l, θ, and ϕ should be determined in a proper manner. This problem will be considered in more details in Sec. 4.

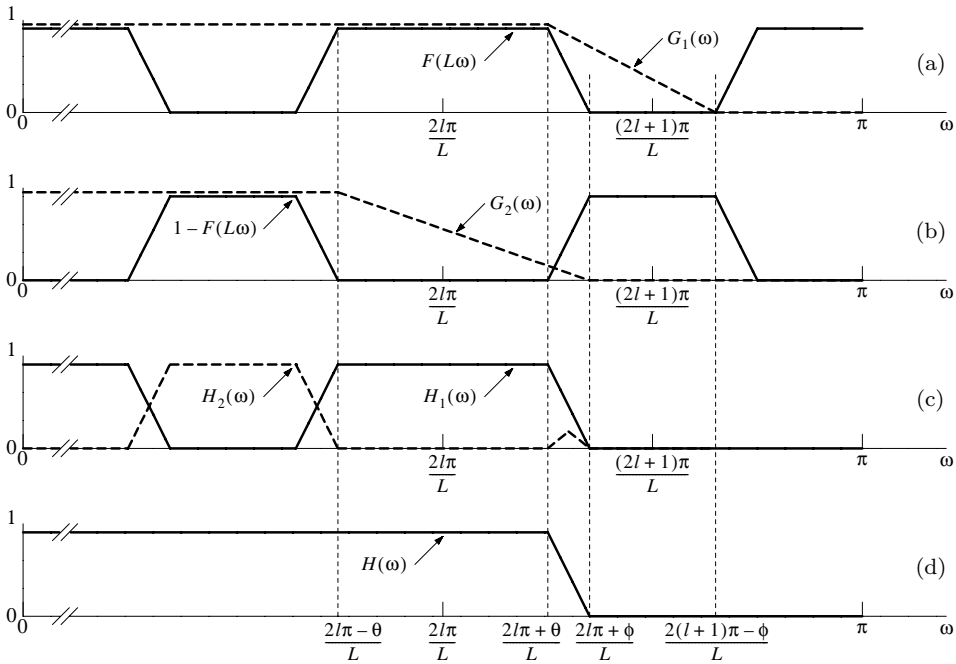

Fig. 3. Case A design of a lowpass filter using the FRM approach.

The widths of these transition bands are $(\phi - \theta)/L$ that is only $1/L$-th that of the prototype filters. This implies that the arithmetic complexity of the periodic transfer functions to provide one of the transition bands is only approximately $1/L$-th that of the optimum conventional (nonperiodic) direct-form FIR filter. Since the order of an FIR filter is roughly inversely proportional to the transition bandwidth, this means that the number of multipliers and adders of the optimum direct-form FIR filter is approximately L times higher to provide the same transition bandwidth. Note that the orders of both the periodic filters and the corresponding optimum direct-form filters are approximately the same, but the direct-form filters do not contain zero-valued impulse-response coefficients.

2.3. *The use of the masking filters $G_1(z)$ and $G_2(z)$ in the original synthesis schemes*

Because of the periodicities of the responses of $F(z^L)$ and $z^{-LN_F/2} - F(z^L)$ they cannot be used alone and there is a need to use the two *masking filters* $G_1(z)$ and $G_2(z)$ as shown in Fig. 1. Their role is two-fold. First, they are designed in such a manner that in the passband of the overall filter, the subresponses $H_1(\omega)$ and $H_2(\omega)$, as given by Eqs. (2b) and (2c), approximate $F(L\omega)$ and $1 - F(L\omega)$, respectively. Hence, $H(\omega) = H_1(\omega)+H_2(\omega)$ (see Eqs. (2a)–(2e) together with Figs. 3 and 4) approximates unity, as is desired. In the stopband, these filters attenuate

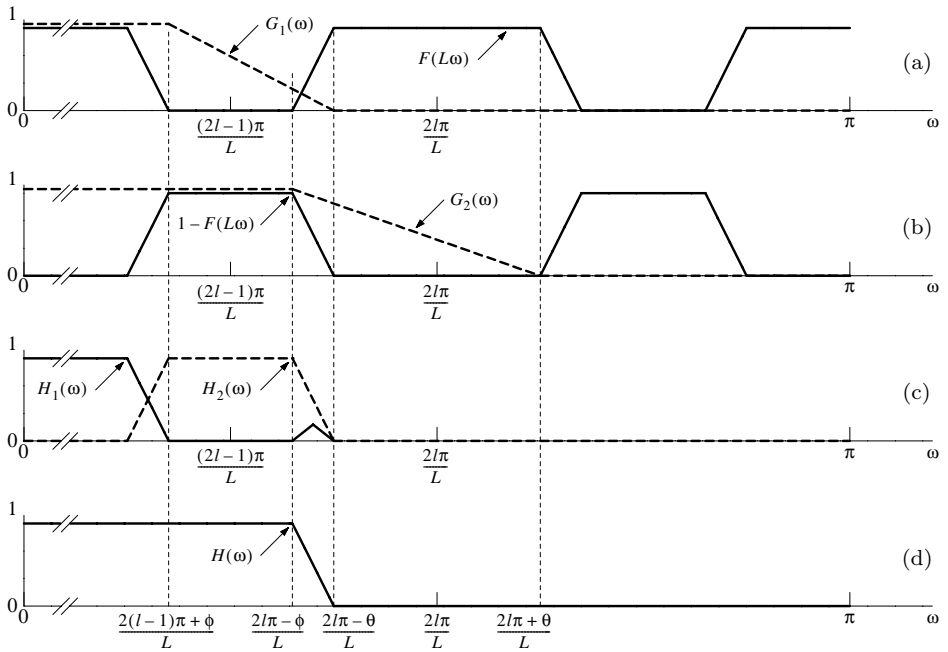

Fig. 4. Case B design of a lowpass filter using the FRM approach.

the extra unwanted passband and transition band regions of $F(L\omega)$ and $1-F(L\omega)$. These goals are achieved for both Case A and Case B designs by selecting the passband and stopband edges of the two lowpass masking filters to be located as shown in Figs. 3 and 4, respectively.

2.4. *Original FRM filter design techniques*

Based on the observations made in Ref. 1, the original design of $H(z)$ with passband and stopband ripples of δ_p and δ_s can be accomplished for both Case A and Case B designs in the following two steps:

Step 1. Design $G_1(z)$ and $G_2(z)$ such that their zero-phase frequency responses approximate unity in their passbands with tolerance less than or equal to $0.9\delta_p$ and zero in their stopbands with tolerance less than or equal to $0.9\delta_s$.

Step 2. Design $F(L\omega)$ such that the overall response $H(\omega)$, as given by Eqs. (2a)–(2e), approximates unity with tolerance less than or equal to δ_p on (see Figs. 3 and 4)

$$\Omega_p^{(F)} = \begin{cases} \left[\dfrac{2l\pi-\theta}{L}\,,\ \dfrac{2l\pi+\theta}{L}\right] & \text{for a Case A design}\,, \\ \left[\dfrac{2(l-1)\pi+\phi}{L}\,,\ \dfrac{2l\pi-\phi}{L}\right] & \text{for a Case B design}\,, \end{cases} \tag{5a}$$

and approximates zero with tolerance less than or equal to δ_s on

$$\Omega_s^{(F)} = \begin{cases} \left[\dfrac{2l\pi+\phi}{L}\,,\ \dfrac{2(l+1)\pi-\phi}{L}\right] & \text{for a Case A design}\,, \\ \left[\dfrac{2l\pi-\theta}{L}\,,\ \dfrac{2l\pi+\theta}{L}\right] & \text{for a Case B design}\,. \end{cases} \tag{5b}$$

Step 1 can be accomplished very fast by using the Remez multiple exchange algorithm.[8] The design of $F(L\omega)$ or $F(\omega)$ at Step 2 of the above two-step procedure can be performed either using linear programming[1,2] or with the aid of the Remez algorithm.[3,4] The order of $G_1(z)$ [$G_2(z)$] can be considerably reduced by allowing larger ripples on those regions of $G_1(z)$ [$G_2(z)$] where $F(L\omega)$ has one of its stopbands [one of its passbands]. As a rule of thumb, the ripples on these regions can be selected to be ten times larger.[1]

3. Proposed Two-Step Design Scheme for Filters with Separate Masking Filters

This section describes the proposed two-step technique for simultaneously designing all the subfilters in the FRM filter in the case where the masking filters are separately implemented. How to select whether to use a Case A design or a Case B design as well as how to properly determine the subfilter orders and the design parameters L, l, θ, and ϕ will be considered in the next section. As will be seen in connection with examples of Sec. 6, the resulting estimated minimum subfilter orders N_F, N_1, and N_2 and the estimated optimum value of L are in the very close vicinity of the actual values minimizing the arithmetic complexity of the overall FRM filter, that is, the number of multipliers and adders required to meet the given overall criteria. This fact considerably reduces the computational workload to arrive at the solution with the lowest arithmetic complexity.

3.1. *Algorithm for finding an initial filter*

Given the subfilter orders (N_F, N_1, and N_2) as well as all the remaining design parameters (ω_p and ω_s, the passband and stopband edges, δ_p and δ_s, the passband and stopband ripples, as well as whether to use a Case A design or a Case B design along with L, l, θ, and ϕ), an initial solution can be found effectively using the following procedure:

Step 1. Set $r = 1$, $\epsilon_G^{(r)} = \epsilon_F^{(r)} = 0$. Determine the parameters of $F^{(r)}(z)$ to minimize

$$\max_{\omega\in[0,\ \theta]\cup[\phi,\ \pi]} |W(\omega)[F^{(r)}(\omega) - D(\omega)]|\,. \tag{6}$$

Here, the first band is the passband, where the desired function $D(\omega)$ and the weighting function $W(\omega)$ are equal to unity. The second band is the stopband,

where $D(\omega)$ is equal to zero and $W(\omega)$ is equal to δ_p/δ_s. In the sequel, the same desired and weighting functions are used.

Step 2. Set $r = r + 1$. Determine the parameters of $G_1^{(r)}(z)$ and $G_2^{(r)}(z)$ to minimize

$$\epsilon_G^{(r)} = \max_{\omega \in [0,\ (1+\alpha_1)\Omega_{p1}] \cup [(1-\alpha_1)\Omega_{s2},\ \pi]} |W(\omega)[H_G^{(r)}(\omega) - D(\omega)]|\,, \tag{7a}$$

where

$$H_G^{(r)}(\omega) = F^{(r-1)}(L\omega)G_1^{(r)}(\omega) + [1 - F^{(r-1)}(L\omega)]G_2^{(r)}(\omega)\,, \tag{7b}$$

$\Omega_{p1} = 2l\pi/L$, and $\Omega_{s2} = (2l+1)\pi/L$ for Case A designs, and $\Omega_{p1} = (2l-1)\pi/L$ and $\Omega_{s2} = 2l\pi/L$ for Case B designs (see Figs. 3 and 4). Here, α_1 is the so-called overlapping constant given by the user.

Step 3. Determine the parameters of $F^{(r)}(z^L)$ to minimize

$$\epsilon_F^{(r)} = \max_{\omega \in [(1-\alpha_2)\Omega_{p1},\ \Omega_{p2}] \cup [\Omega_{s1},\ (1+\alpha_2)\Omega_{s2}]} |W(\omega)[H_F^{(r)}(\omega) - D(\omega)]|\,, \tag{8a}$$

where

$$H_F^{(r)}(\omega) = F^{(r)}(L\omega)G_1^{(r)}(\omega) + [1 - F^{(r)}(L\omega)]G_2^{(r)}(\omega)\,, \tag{8b}$$

$\Omega_{p2} = (2l\pi + \theta)/L$, and $\Omega_{s1} = (2l\pi + \phi)/L$ for Case A designs, and $\Omega_{p2} = (2l\pi - \phi)/L$ and $\Omega_{s1} = (2l\pi - \theta)/L$ for Case B designs (see Figs. 3 and 4). Here, Ω_{p1} and Ω_{s2} are the same as at Step 2 and α_2 is another overlapping constant specified by the user.

Step 4. If $|\epsilon_G^{(r)} - \epsilon_G^{(r-1)}| \le \Delta$ and $|\epsilon_F^{(r)} - \epsilon_F^{(r-1)}| \le \Delta$, where Δ is a prescribed tolerance, then stop. Otherwise, go to Step 2.

The basic idea in the above algorithm is to share the frequency-response-shaping responsibilities in such a manner that $G_1(z)$ and $G_2(z)$ concentrate mainly on generating the desired response on $[0,\ \Omega_{p1}]$ and $[\Omega_{s2},\ \pi]$, whereas $F(z^L)$ concentrates on the regions $[\Omega_{p1},\ \Omega_{p2}]$ and $[\Omega_{s1},\ \Omega_{s2}]$ (see Figs. 3 and 4). It has turned out to be beneficial to use the overlapping constants α_1 and α_2 in the above algorithm such that the above-mentioned regions slightly overlap. This makes the convergence of the algorithm significantly faster. In most cases, good selections for these constants are $\alpha_1 = \alpha_2 = 0.01$.

Step 1 in the above algorithm can be accomplished very fast by using the Remez multiple exchange algorithm,[8] whereas Steps 2 and 3[c] can be implemented using linear programming. In order to arrive at a good enough overall solution, only

[c]In Ref. 4, the Remez multiple exchange algorithm[8] has been exploited for optimizing the zero-phase frequency response of $F(z^L)$ in order to make the overall design procedure faster than in the original FRM approaches.[1,2] This is due to the fact that the roles of the masking filters $G_1(z)$ and $G_2(z)$ are well defined. However, in the proposed synthesis scheme, their roles are totally different. Therefore, it is recommended to use linear programming for designing $F(z^L)$ at Step 3. Future work is devoted to making the design of $F(z^L)$ faster by properly using the Remez algorithm or a proper combination of linear programming and the Remez algorithm.

$8(N_1 + N_2)$ [$8N_F$] grid points are needed at Step 2 [Step 3]. It should be pointed out that roughly 300 iterations of the above algorithm are required. This is mainly due to the fact that the maximum magnitude value of $F(z^L)$ is gradually changing in the above algorithm. How to adjust this maximum value to a proper level by using a constrained optimization algorithm will be considered in connection with examples of Sec. 6. Even though the required number of iterations is large, the overall computation time is not long due to the fact that each iteration can be performed very fast.

There exist the following two attractive facts in the above algorithm. First, as already mentioned in the beginning of this section, L as well as the orders of $F(z^L)$, $G_1(z)$, and $G_2(z)$ minimizing the overall filter complexity can be estimated very accurately according to the discussion of Sec. 4 so that the overall two-step optimization technique proposed in this section has to be applied a very few times. Second, it is very straightforward to determine, with the aid of the above algorithm, the minimum filter orders yielding a satisfactory result after applying further optimization. This goal is achieved if, after the convergence of the above algorithm, both of the resulting $\epsilon_G^{(r)}$ and $\epsilon_F^{(r)}$ are very close to δ_p.[d] In most cases, a good candidate is obtained when one of them is slightly less than δ_p and the remaining one is slightly larger than δ_p.

3.2. *Further optimization*

The solution obtained using the above algorithm can be further improved with the aid of an efficient unconstrained nonlinear optimization technique, as will be described in Appendix A.

4. Practical Filter Synthesis

In practice, ω_p and ω_s are given and L, l, θ, and ϕ must be determined to give the desired solution with the minimum arithmetic complexity. For a given value of L, either a Case A design or a Case B design (not both) can be used provided that L is not too large.[1–3] A Case A design is applicable if l, θ, and ϕ are determined as[e]

$$l = \left\lfloor \frac{L\omega_p}{2\pi} \right\rfloor , \quad \theta = L\omega_p - 2l\pi , \quad \text{and} \quad \phi = L\omega_s - 2l\pi , \tag{9a}$$

and the resulting θ and ϕ satisfy $0 \le \theta < \phi \le \pi$. Similarly, a Case B design can be used if l, θ, and ϕ are determined as[f]

$$l = \left\lceil \frac{L\omega_s}{2\pi} \right\rceil , \quad \theta = 2l\pi - L\omega_s , \quad \text{and} \quad \phi = 2l\pi - L\omega_p , \tag{9b}$$

[d] $\epsilon_G^{(r)}$, as given by Eq. (7) [$\epsilon_F^{(r)}$, as given by Eq. (8)], has been constructed such that if it achieves exactly the specified value of δ_p, then the passband and stopband ripples provided by $G_1(z)$ and $G_2(z)$ [by $F(z^L)$] for the overall response are exactly the specified values of δ_p and δ_s.

[e] $\lfloor x \rfloor$ stands for the largest integer that is smaller than or equal to x.

[f] $\lceil x \rceil$ stands for the smallest integer that is larger than or equal to x.

and the resulting θ and ϕ satisfy $0 \leq \theta < \phi \leq \pi$. If $\theta = 0$ or $\phi = \pi$, then the resulting specifications for $F(\omega)$ are meaningless and the corresponding value of L cannot be used.

The remaining problem is to determine L to minimize the number of multipliers, that is, $N_F/2 + 1 + \lfloor (N_1 + 2)/2 \rfloor + \lfloor (N_2 + 2)/2 \rfloor$ when the coefficient symmetries are exploited. For both the original approaches[1–4] and the proposed approach, it has turned out that a good estimate for N_F is the minimum order for the zero-phase frequency response of $F(z)$ to stay within $1 \pm \delta_p$ ($\pm\delta_s$) on $[0,\ \theta]$ ($[\phi,\ \pi]$). For the best filters designed using the original FRM approach, good estimates for N_1 and N_2 are the minimum orders for the zero-phase frequency responses of $G_1(z)$ and $G_2(z)$ to stay within the same limits in their passband and stopband regions (cf. Step 1 in Sec. 2.4).

For the filters designed using the proposed technique, good estimates for N_1 and N_2 have turned out to be 60% of those of the original designs. Based on this observation, it can be shown that the values of L giving the lowest arithmetic complexities can be found in the near vicinity of

$$L_{\text{opt}} = \frac{1}{\sqrt{1.2(\omega_s - \omega_p)/\pi}}\,. \tag{10}$$

The above equation can be derived in a manner similar to that used in Refs. 2 and 3 for the original design techniques. The best results are usually obtained at those values of L where $\theta + \phi$ is close to π.[2,3] In this case, the transition bandwidths of both $G_1(z)$ and $G_2(z)$ are approximately equal to $(\theta + \phi)/L$, thereby making N_1 and N_2 approximately equal.

5. Two-Step Design Scheme for Filters with a Common Part for the Masking Filters

Due to the fact that the magnitude responses for the masking filters $G_1(z)$ and $G_2(z)$ after the simultaneous optimization are very similar (see, e.g., Fig. 6[g] in Ref. 6 or Fig. 8 in this contribution), it is beneficial to use a common filter part $G_3(z)$ for constructing the masking filters as shown in Fig. 5. In this case, the overall transfer function is given by

$$H(z) = \Big[F(z^L)G_1(z) + \big[z^{-LN_F/2} - F(z^L)\big]G_2(z)\Big]\,G_3(z)\,, \tag{11a}$$

where $F(z^L)$ as well as $G_1(z)$ and $G_2(z)$ are given by Eq. (1) and

$$G_3(z) = \sum_{n=0}^{N_3} g_3(n) z^{-n} \tag{11b}$$

with $g_3(n)$ possessing an even symmetry. Hence, $G_3(\omega)$, the zero-phase frequency response of $G_3(z)$, can be expressed in a form similar to that of Eq. (2e). For this

[g]It should be noted that in this figure, $N_F = 124$, instead of $N_F = 122$, has been used.

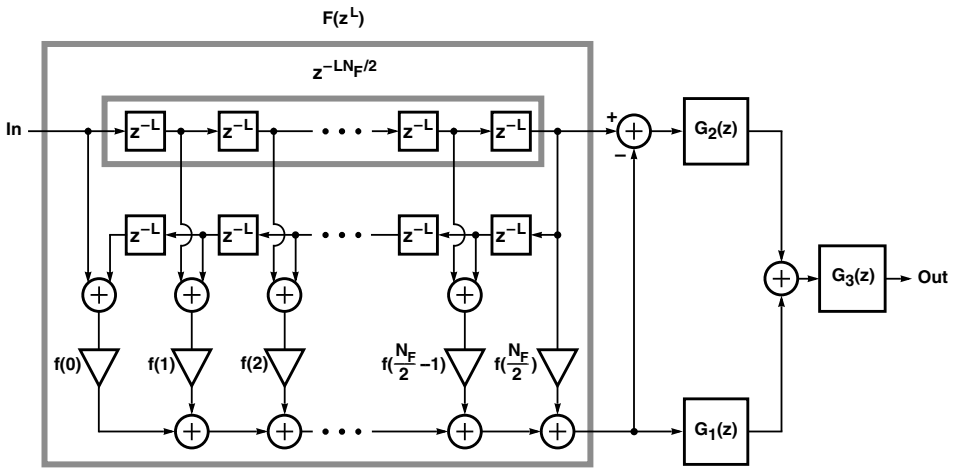

Fig. 5. Implementation for a filter synthesized using the generalized FRM approach. In this implementation, the masking filters are constructed using a common filter part $G_3(z)$.

generalized FRM approach, it has turned out that the solutions giving the lowest arithmetic complexities are usually obtained by selecting one of the subfilters $G_1(z)$ or $G_2(z)$ in Fig. 5 to be a pure delay. In order to generate a linear-phase overall filter, this implies that the order of the remaining one is two times this delay. In these two cases, the overall zero-phase frequency response is expressible as

$$H(\omega) = \begin{cases} F(L\omega)G_3(\omega) + [1 - F(L\omega)]G_2(\omega)G_3(\omega) & \text{if } G_1(z) \text{ is a pure delay}, \\ F(L\omega)G_1(\omega)G_3(\omega) + [1 - F(L\omega)]G_3(\omega) & \text{if } G_2(z) \text{ is a pure delay}. \end{cases} \tag{12}$$

The design algorithm for generating $F(z^L)$ as well as $G_1(z)$, $G_2(z)$, and $G_3(z)$ to meet the given overall criteria in the above-mentioned two cases can be carried out as follows:

Step 1. Design $F(z^L)$ and the $G_k(z)$'s for $k = 1, 2$ using the two-step approach described in Sec. 3.

Step 2. If $N_1 < N_2$, then select $G_3(z) \equiv G_1(z)$. Furthermore, select $N_2 \equiv N_2 - N_1$, $G_1(z) \equiv z^{-N_2/2}$ ($N_1 = 0$), and select the starting order of $G_2(z)$ to be N_2.[h] Otherwise, select $G_3(z) \equiv G_2(z)$, $N_1 \equiv N_1 - N_2$, $G_2(z) \equiv z^{-N_1/2}$ ($N_2 = 0$), and select the starting order of $G_1(z)$ to be N_1.

Step 3. If $G_1(z) = z^{-N_2/2}$, then use an iterative algorithm similar to that used in Sec. 3.1 for alternately designing $F(z^L)$ as well as $G_2(z)$ and $G_3(z)$. In this algorithm, an even integer N_2 is increased until the overall filter meets the given criteria. Otherwise, use the similar algorithm for alternately designing $F(z^L)$ as well

[h]According to the discussion of Sec. 2.1, this corresponds to the case where N_1, the order of $G_1(z)$, is zero and the additional delay term $z^{-N_2/2}$ is needed to make the delays of $G_1(z)$ and $G_2(z)$ equal.

as $G_1(z)$ and $G_3(z)$ ($G_2(z) = z^{-N_1/2}$). Similarly, an even integer N_1 is gradually increased for finding its minimum value to meet the given overall specifications.
Step 4. Apply an efficient unconstrained optimization algorithm, as described in Appendix A, for simultaneously optimizing all the subfilters for further improving the filter performance using the result of Step 3 as a start-up solution.

The design of $F(z^L)$ at Step 3 in the above algorithm can be performed as at Step 3 in the algorithm described in Sec. 3.1 by using the following substitutions:

$$G_1(\omega) \equiv \begin{cases} G_3(\omega) & \text{if } G_1(z) \text{ is a pure delay}, \\ G_1(\omega)G_3(\omega) & \text{if } G_2(z) \text{ is a pure delay}, \end{cases} \tag{13a}$$

and

$$G_2(\omega) \equiv \begin{cases} G_2(\omega)G_3(\omega) & \text{if } G_1(z) \text{ is a pure delay}, \\ G_3(\omega) & \text{if } G_2(z) \text{ is a pure delay}. \end{cases} \tag{13b}$$

How to properly design $G_1(z)$, $G_2(z)$, and $G_3(z)$ at Step 3 in the above algorithm will be described in Appendix B.

6. Numerical Examples

This section illustrates, by means of an example taken from the literature, the efficiency of the filters resulting when applying the proposed techniques compared with those obtained using the original design schemes.[1–4]

6.1. *Filter specifications*

Consider the specifications[3,4]: $\omega_p = 0.4\pi$, $\omega_s = 0.402\pi$, $\delta_p = 0.01$, and $\delta_s = 0.001$. For the optimum conventional direct-form FIR filter, the minimum order to meet the given criteria is 2541, requiring 1271 multipliers and 2541 adders when the coefficient symmetry is exploited.

6.2. *Filters resulting when using the original design schemes*

For the original design techniques,[1–4] $L = 16$ minimizes the number of multipliers required in the implementation.[3,4] For $L = 16$, the overall filter is a Case A design with $l = 3$, $\theta = 0.4\pi$, and $\phi = 0.432\pi$. The minimum orders for $G_1(z)$, $G_2(z)$, and $F(z)$ to meet the given specifications are $N_1 = 70$, $N_2 = 98$, and $N_F = 162$, respectively. The overall number of multipliers and adders for this design are 168 and 332,[i] respectively, that are 13% of those required by an equivalent conventional direct-form design (1271 and 2541). The overall filter order is 2690 that is only 6% higher than that of the direct-form design (2541).

[i]The two additional adders in the structure of Fig. 1 are included in this figure. In the sequel, the same will be done in the case of the proposed optimized filter with separable masking filters as well as in the case where the masking filters share a common part as shown in Fig. 5.

6.3. *Optimized filters with separate masking filters for* $L = 16$

For $L = 16$, the best[j] solution resulting when using the proposed synthesis scheme with separate masking filters is obtained by $N_1 = 47$, $N_2 = 57$, and $N_F = 160$. For this filter, the number of multipliers and adders are 134 and 266, respectively, that are approximately 80% of those of the original design. Furthermore, when compared with the original design, the overall filter order reduces from 2690 to 2617.

According to the discussion of Sec. 4, the minimum estimated even order for $F(z)$ and the minimum estimated orders for $G_1(z)$ and $G_2(z)$ are $N_F = 160$, $N_1 = 42$, and $N_2 = 59$, respectively. Since the orders of both $G_1(z)$ and $G_2(z)$ should be even or odd, it was first tried to use $N_F = 160$ and $N_2 = 59$ and to find the minimum odd order N_1 such that the algorithm of Sec. 3.1 gives a satisfactory overall solution. This resulted in $N_1 = 45$, $\delta_p = 10\delta_s = 0.00998$ for the region mainly taken care of $F(z^L)$, and $\delta_p = 10\delta_s = 0.00971$ for the region mainly taken care of $G_1(z)$ and $G_2(z)$. What was left was to gradually increase N_1 by two and to decrease N_2 by two in order to decrease the overall FRM filter order. The limit was achieved by $N_1 = 47$ and $N_2 = 57$, giving $\delta_p = 10\delta_s = 0.01000$ for the region of $F(z^L)$ and $\delta_p = 10\delta_s = 0.00988$ for the region of $G_1(z)$ and $G_2(z)$. For this design, the maximum magnitude value of $F(z^L)$ and the value at the zero frequency are approximately 2.93 and 2.54, respectively. The further optimization resulted in $\delta_p = 10\delta_s = 0.00999$.[k]

There are the following two important properties of the proposed FRM filters to be pointed out. First, the subfilter orders estimated according to the discussion of Sec. 4 are very close to the orders minimizing the arithmetic complexity, implying that the two-step optimization technique described in Sec. 3 has to be carried out a very few times. Second, as will be seen in the following subsections, there are numerous solutions giving approximately the same result. These solutions differ from each other in the sense that independent of the maximum value of the zero-phase frequency response of $F(z^L)$, practically the same passband and stopband ripples for the overall FRM filter are achieved.

6.4. *Optimized filters with separate masking filters for* $L = 21$

For the proposed filters with separate masking filters, the overall number of multipliers is minimized by $L = 21$ [the value obtained using Eq. (10)]. This filter is a Case A design with $l = 4$, $\theta = 0.4\pi$, and $\phi = 0.442\pi$. Proceeding in the same manner as for $L = 16$, the best solution is obtained by $N_1 = 55$, $N_2 = 77$, and

[j]The measure of goodness is the overall number of multipliers. If there exist several solutions requiring the same minimum number of multipliers, then, first, the solution with the minimum value of N_F is selected and, second, the one having a lower value for the maximum of N_1 and N_2 is selected. In this case, the overall filter order, as given by $LN_F + \max\{N_1, N_2\}$, is minimized.

[k]If an FRM filter with a lower arithmetic complexity is desired to be generated, then it is worth trying to decrease N_F while keeping the sum of $N_1 + N_2$ the same or to decrease $\lfloor (N_1 + 2)/2 \rfloor + \lfloor (N_2 + 2)/2 \rfloor$ while keeping N_F the same. However, these alternatives gave no satisfactory results.

$N_F = 122$. In this case, the orders estimated according to the discussion of Sec. 4 are $N_1 = 55$, $N_2 = 76$, and $N_F = 122$. Hence, the estimated order for N_2 differs only by one, while the remaining estimated orders are directly the minimum orders. The procedure of Sec. 3.1 resulted in $\delta_p = 10\delta_s = 0.01001$ for the region of $F(z^L)$ and $\delta_p = 10\delta_s = 0.00941$ for the region of $G_1(z)$ and $G_2(z)$. For this design, the maximum magnitude value of $F(z^L)$ and the value at the zero frequency are approximately 2.52 and 2.75, respectively. This filter requires 129 multipliers and 256 adders that are approximately 77% of those of the original best design for $L = 16$.

In order to illustrate that there exist various solutions with practically the same ripple values, further optimization was performed subject to the following two constraints,[l] namely, $\sum_{n=0}^{N_F} f(n) = 10$ and $\sum_{n=0}^{N_F} f(n) = 1.2$. For $\sum_{n=0}^{N_F} f(n) = 10$, Figs. 6–8 show the responses for $F(L\omega)$ and $1 - F(L\omega)$, $F(\omega)$ and $1 - F(\omega)$, and the magnitude responses for $G_1(z)$ and $G_2(z)$, respectively. The responses $H_1(\omega) = F(L\omega)G_1(\omega)$ and $H_2(\omega) = [1 - F(L\omega)]G_2(\omega)$ are shown in Fig. 9, whereas the overall magnitude response for $H(z) = H_1(z) + H_2(z)$ is depicted in Fig. 10. Two interesting observations can be made from these figures. First, $F(L\omega)$ and $F(L\omega)G_1(\omega)$ in the passband region [$1 - F(L\omega)$ and $[1 - F(L\omega)]G_2(\omega)$ in the passband region] varies approximately between -9.5 and 11.5 [-10.5 and 10.5].[m] Second, the magnitude responses for $G_1(z)$ and $G_2(z)$ are very similar.

Similar characteristics for $\sum_{n=0}^{N_F} f(n) = 1.2$ are shown in Figs. 11–13. As shown in Fig. 12, the masking filters for this FRM filter are very different. From the implementation point of view, this latter FRM filter is preferable. This is due to the fact that the impulse-response values of $F(z^L)$ are significantly smaller.

6.5. *Optimized filters with a common part for the masking filters*

When simultaneously optimizing the subfilters in the case where the masking filters share a common filter part, the overall number of multipliers is minimized also by $L = 21$. Using the best design with separate masking filters as a start-up solution at Step 2 in the algorithm of Sec. 5, the orders for $F(z)$, $G_1(z)$, $G_2(z)$, and $G_3(z)$ became 122, 0 ($G_1(z) = z^{-N_2/2} = z^{-11}$), 22, and 55, respectively. For this design, the simultaneous optimization of all the subfilters resulted in $\delta_p = 10\delta_s = 0.03529$. Since the order of $G_2(z)$ should be even, N_2 was gradually increased by two until the overall filter met the given specifications. This goal was achieved by $N_2 = 46$ ($G_1(z) = z^{-N_2/2} = z^{-23}$), giving $\delta_p = 10\delta_s = 0.00999$. For this FRM filter,

[l]The optimization was performed as described in Appendix A with the exception that there exists now a linear constraint. The resulting problem can be solved conveniently using the function `fminimax` from the optimization toolbox provided by MathWorks, Inc.[9]

[m]If the peak scaling and two's complement arithmetic are desired to be used and $G_1(z)$ and $G_2(z)$ share their delays by using the transposed direct-form structure exploiting the coefficient symmetry in Fig. 1, then there exist two alternatives for the scaling. In the first alternative, the overall input is divided by a constant β being the maximum value of $F(L\omega)$ and the coefficients of $G_1(z)$ and $G_2(z)$ are multiplied by β. In the second alternative, the coefficients $f(n)$ in Fig. 1 as well as the output of the delay line $z^{-LN_F/2}$ are divided by β.

the optimization was performed in such a manner that the maximum magnitude values of $F(z^L)$ and $G_3(z)$ became approximately the same, that is, 2.85. This filter requires 114 multipliers and 227 adders that are approximately 88% of those obtained by simultaneously optimizing all the subfilters without the common part for the masking filters.

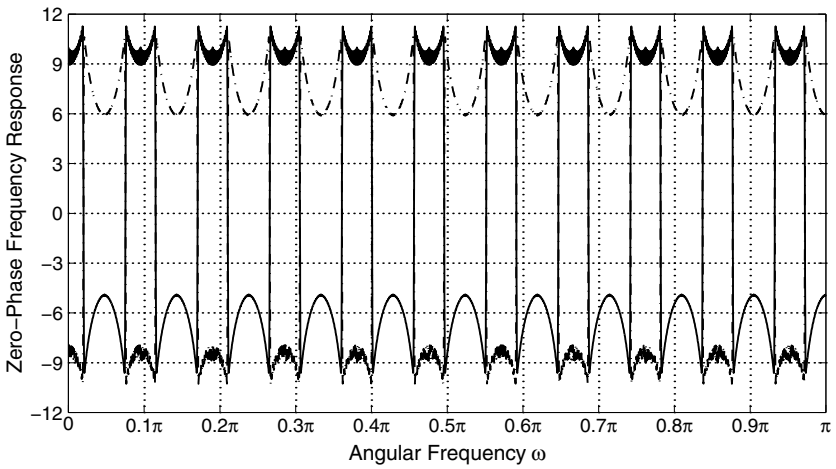

Fig. 6. Responses for $F(L\omega)$ (——) and $1 - F(L\omega)$ $(- \cdot -)$ for the best proposed filter with separate masking filters for $L = 21$ and $\sum_{n=0}^{N_F} f(n) = 10$.

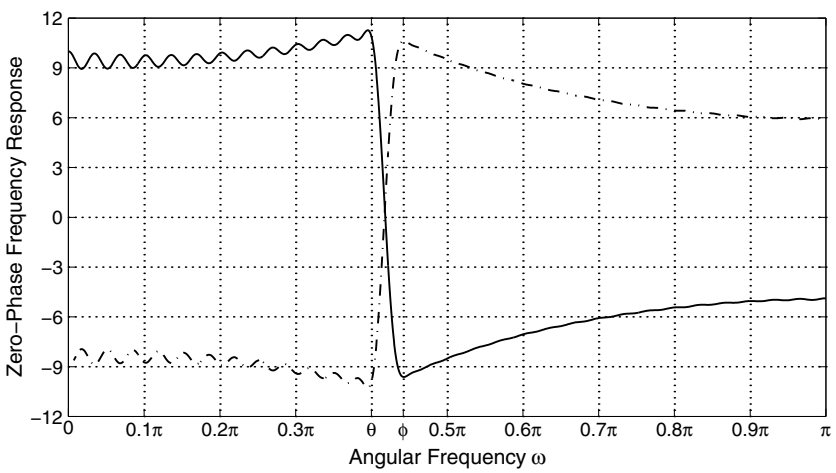

Fig. 7. Responses for $F(\omega)$ (——) and $1 - F(\omega)$ $(- \cdot -)$ for the best proposed filter with separate masking filters for $L = 21$ and $\sum_{n=0}^{N_F} f(n) = 10$.

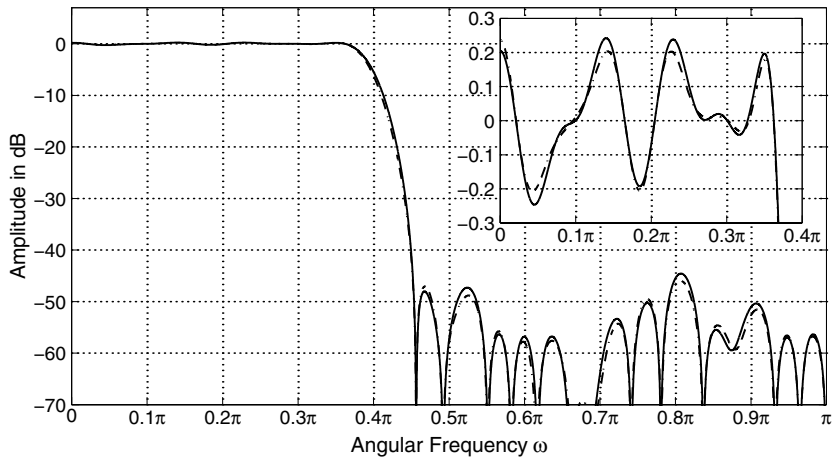

Fig. 8. Magnitude responses for $G_1(z)$ (——) and $G_2(z)$ $(- \cdot -)$ for the best proposed filter with separate masking filters for $L = 21$ and $\sum_{n=0}^{N_F} f(n) = 10$.

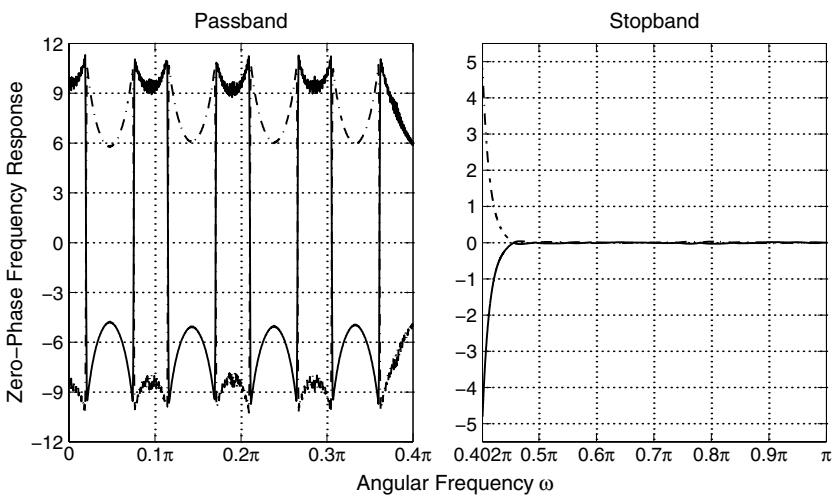

Fig. 9. Responses for $F(L\omega)G_1(\omega)$ (——) and $[1 - F(L\omega)]G_2(\omega)$ $(- \cdot -)$ for the best proposed filter with separate masking filters for $L = 21$ and $\sum_{n=0}^{N_F} f(n) = 10$.

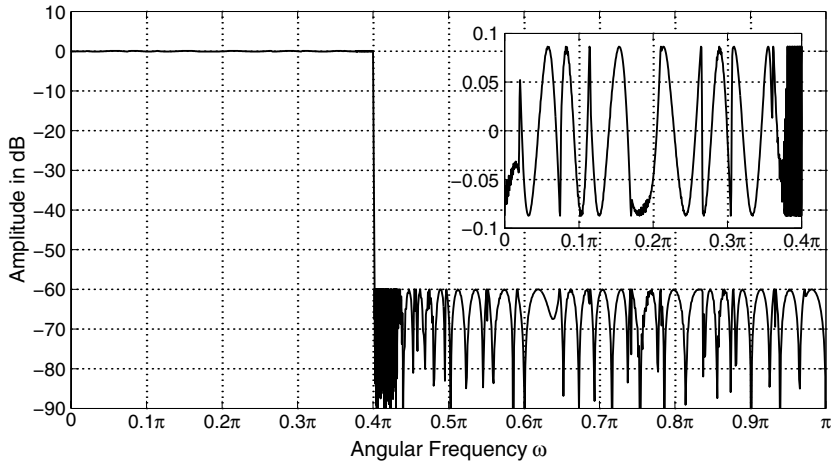

Fig. 10. Magnitude response for the best proposed overall filter with separate masking filters for $L = 21$ and $\sum_{n=0}^{N_F} f(n) = 10$.

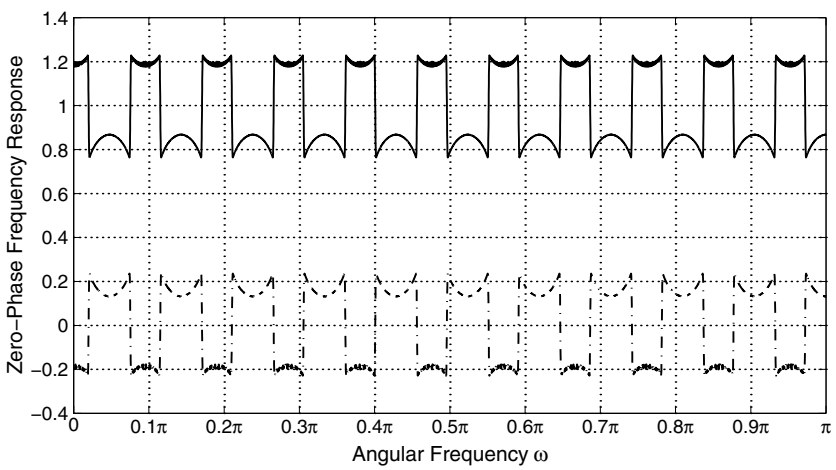

Fig. 11. Responses for $F(L\omega)$ (——) and $1 - F(L\omega)$ (– · –) for the best proposed filter with separate masking filters for $L = 21$ and $\sum_{n=0}^{N_F} f(n) = 1.2$.

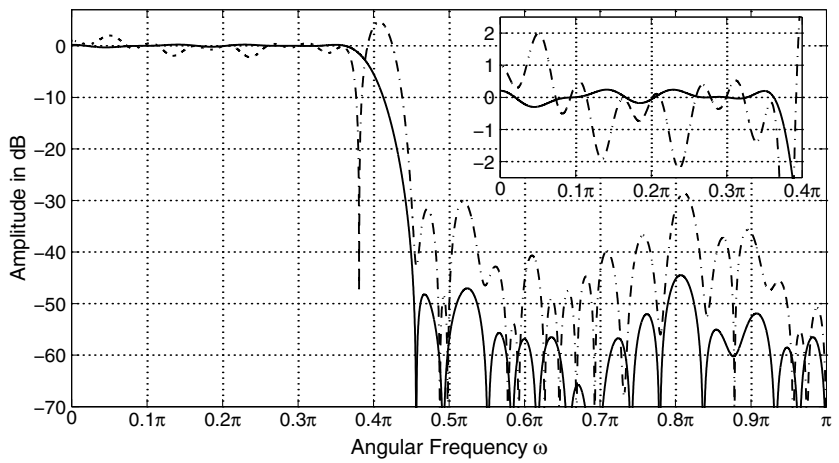

Fig. 12. Magnitude responses for $G_1(z)$ (——) and $G_2(z)$ $(- \cdot -)$ for the best proposed filter with separate masking filters for $L = 21$ and $\sum_{n=0}^{N_F} f(n) = 1.2$.

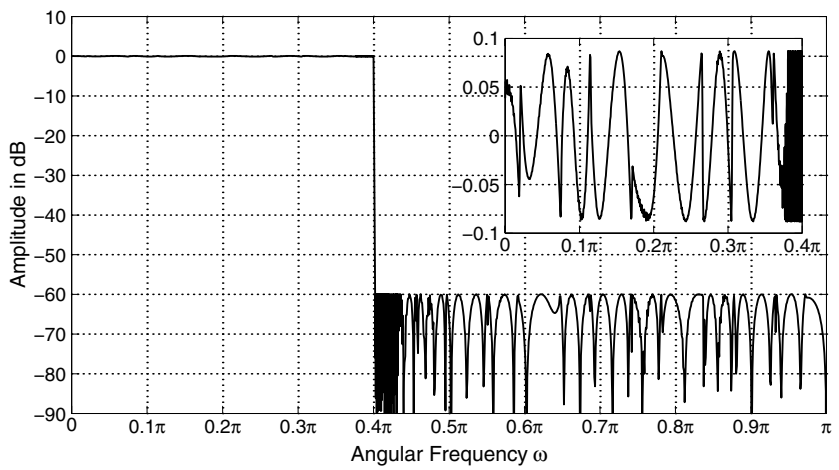

Fig. 13. Magnitude response for the best proposed overall filter with separate masking filters for $L = 21$ and $\sum_{n=0}^{N_F} f(n) = 1.2$.

For this FRM design, Figs. 14 and 15 show the responses for $F(L\omega)$ and $1 - F(L\omega)$ and the magnitude responses for $G_2(z)$ and $G_3(z)$, respectively. The zero-plots for $G_2(z)$ and $G_3(z)$ are shown in Fig. 16, whereas the overall magnitude response for $H(z)$ is depicted in Fig. 17.

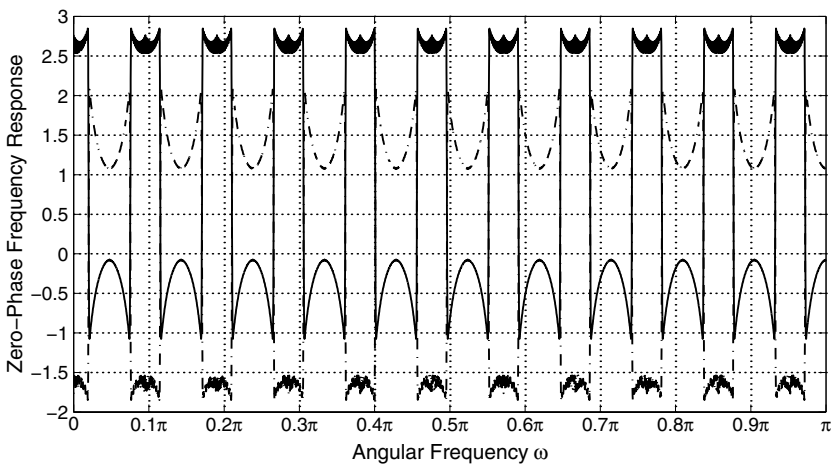

Fig. 14. Responses for $F(L\omega)$ (——) and $1 - F(L\omega)$ ($- \cdot -$) for the best proposed filter with a common part for the masking filters for $L = 21$.

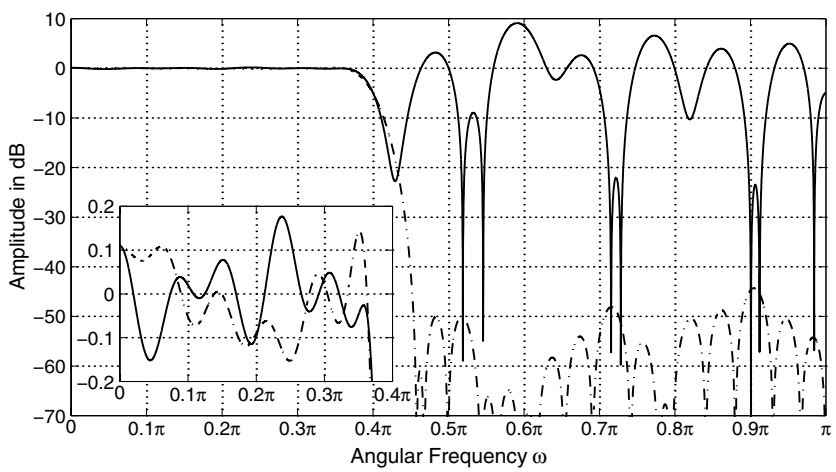

Fig. 15. Magnitude responses for $G_2(z)$ (——) and $G_3(z)$ ($- \cdot -$). $G_1(\omega) \equiv 1$ since $G_1(z) = z^{-23}$.

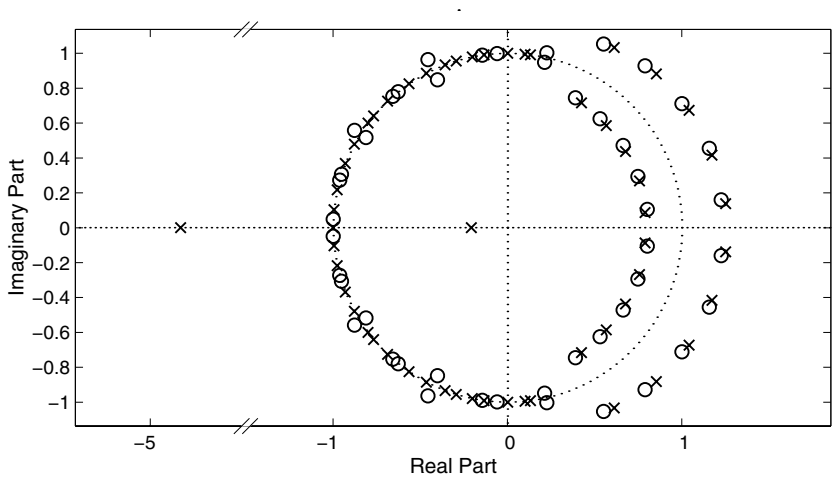

Fig. 16. Zero-plots for the masking filters. The circles and crosses show the zero locations of $G_2(z)$ and $G_3(z)$, respectively.

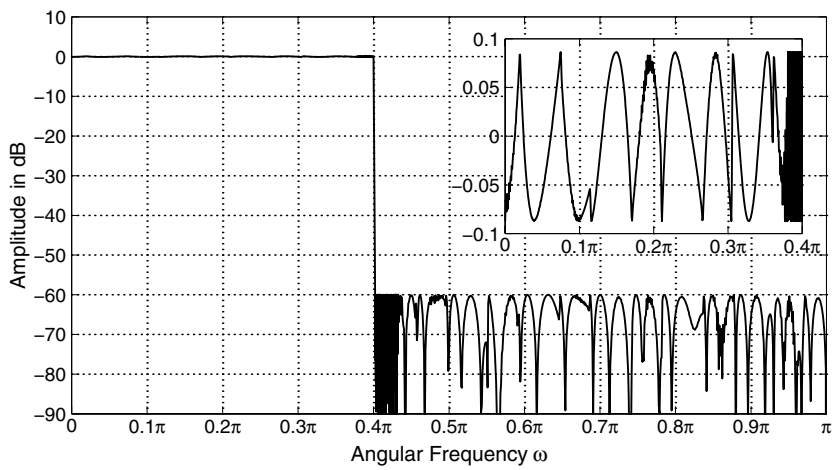

Fig. 17. Magnitude response for the best proposed overall filter with a common part for the masking filters for $L = 21$.

Table 1. Summary of filter designs in the example under consideration.

Method	L	N_F	N_1	N_2	N_3	N_M
Conventional direct-form filter	1	2541	–	–	–	1271
Original[3,4]	16	162	70	98	–	168
Separate masking filters	16	160	47	57	–	134
Separate masking filters	21	122	55	77	–	129
Common filter part	21	122	0	46	55	114

6.6. *Summary of the filter designs*

Some of the characteristics for the filters designed in this section using various algorithms are summarized in Table 1, where N_M denotes the number of multipliers required to implement the overall filter. The optimized impulse-response values of $F(z)$, $G_1(z)$, and $G_2(z)$ for the best proposed filter with separate masking filters for $L = 21$ and $\sum_{n=0}^{N_F} f(n) = 1.2$ as well as the optimized impulse-response values of $F(z)$, $G_2(z)$, and $G_3(z)$ for the best proposed filter with a common part for the masking filters are given in Tables C.1–C.3 and C.4–C.6 in Appendix C, respectively.

7. Conclusions

A two-step optimization technique has been proposed for considerably reducing the arithmetic complexity of linear-phase FRM based FIR filters in two cases, namely, the case with separately implemented masking filters and the case where the two masking filters share a common filter part. In both cases, an initial filter is generated at the first step with the aid of a simple iterative algorithm. At the second step, this start-up design is improved using an efficient unconstrained nonlinear optimization. An example taken from the literature has shown that in the case of separate masking filters the number of adders and multipliers for the optimized filter is less than 80% compared to that obtained using the original design techniques where all the subfilters are separately designed. An additional reduction of more than 10% is achievable by using a common part for the masking filters. It has been observed, by using other filter criteria, that these reductions are approximately valid also for other specifications. Future work is devoted to characterizing in more details the behavior of the resulting optimized filters as well as to applying similar techniques to the multistage FRM approach. Furthermore, for both above-mentioned FRM filter classes, the proposed design schemes will be modified to give directly the best solution after specifying the filter criteria.

Acknowledgment

This work was supported by the Academy of Finland, project No. 44876 (Finnish Centre of Excellence Program (2000–2005)).

Appendix A

This appendix shows how to properly improve the performance of the initial filters generated in Secs. 3 and 5.

In order to treat all the problems considered in Secs. 3 and 5 in a similar manner, the problems under consideration are categorized into the following types:

Type I. $H(z)$ is implemented according to Fig. 1, where $F(z^L)$ is of even order N_F in z^L, whereas $G_1(z)$ and $G_2(z)$ are of orders N_1 and N_2 such that both N_1 and N_2 are either even or odd integers.
Type II. $H(z)$ is implemented according to Fig. 5, where $F(z^L)$ is of even order N_F in z^L, $G_2(z)$ is of even order N_2, $G_1(z) = z^{-N_2/2}$, and $G_3(z)$ is of order N_3.
Type III. $H(z)$ is implemented according to Fig. 5, where $F(z^L)$ is of even order N_F in z^L, $G_1(z)$ is of even order N_1, $G_2(z) = z^{-N_1/2}$, and $G_3(z)$ is of order N_3.

For all these types, the zero-phase frequency response of $H(z)$ is expressible as

$$H(\Phi,\omega) = \begin{cases} F(L\omega)G_1(\omega) + [1 - F(L\omega)]G_2(\omega) & \text{for Type I}\,, \\ F(L\omega)G_3(\omega) + [1 - F(L\omega)]G_2(\omega)G_3(\omega) & \text{for Type II}\,, \\ F(L\omega)G_1(\omega)G_3(\omega) + [1 - F(L\omega)]G_3(\omega) & \text{for Type III}\,, \end{cases} \tag{A.1a}$$

where $F(\omega)$ is given by Eq. (2d), the $G_k(\omega)$'s for $k = 1, 2, 3$ are given by Eq. (2e), and Φ is the parameter vector containing the adjustable impulse-response values and is given by

$$\Phi = \begin{cases} \left[f(0), \ldots, f(\frac{N_F}{2}), g_1(0), \ldots, g_1\lfloor\frac{N_1}{2}\rfloor, g_2(0), \ldots, g_2\lfloor\frac{N_2}{2}\rfloor\right] & \text{for Type I}\,, \\ \left[f(0), \ldots, f(\frac{N_F}{2}), g_2(0), \ldots, g_2(\frac{N_2}{2}), g_3(0), \ldots, g_3\lfloor\frac{N_3}{2}\rfloor\right] & \text{for Type II}\,, \\ \left[f(0), \ldots, f(\frac{N_F}{2}), g_1(0), \ldots, g_1(\frac{N_1}{2}), g_3(0), \ldots, g_3\lfloor\frac{N_3}{2}\rfloor\right] & \text{for Type III}\,. \end{cases} \tag{A.1b}$$

The common problem including the above three types is to find the adjustable parameter vector Φ to minimize

$$\max_{\omega\in[0,\ \omega_p]\cup[\omega_s,\ \pi]} |E(\Phi,\omega)|\,, \tag{A.2a}$$

where

$$E(\Phi,\omega) = W(\omega)[H(\Phi,\omega) - D(\omega)]\,, \tag{A.2b}$$

ω_p and ω_s are given by Eq. (3) [Eq. (4)] for a Case A design [a Case B design],

$$D(\omega) = \begin{cases} 1 \text{ for } \ \omega \in [0,\ \omega_p]\,, \\ 0 \text{ for } \ \omega \in [\omega_s,\ \pi]\,, \end{cases} \tag{A.2c}$$

and

$$W(\omega) = \begin{cases} 1 & \text{for } \omega \in [0,\ \omega_p]\,, \\ \dfrac{\delta_p}{\delta_s} & \text{for } \omega \in [\omega_s,\ \pi]\,. \end{cases} \tag{A.2d}$$

In order to solve this problem, the passband and stopband regions are discretized into the frequency points $\omega_i \in [0,\ \omega_p]$ for $i = 1, 2, \ldots, L_p$ and $\omega_i \in [\omega_s,\ \pi]$ for $i = L_p + 1, L_p + 2, \ldots, L_p + L_s$. The resulting discrete minimax problem is to find Φ to minimize

$$\epsilon = \max_{1 \le i \le L_p + L_s} |E(\Phi, \omega_i)|\,. \tag{A.3}$$

This problem can be solved using an effective unconstrained nonlinear optimization algorithm. For this purpose, the function `fminimax` from the optimization toolbox provided by MathWorks, Inc. has been used.[9] When using this function, the user has to provide a function which evaluates the objective function, that is, the error function to be minimized at the given frequency points as well as the gradients of the objective function with respect to the adjustable parameters. The solution meeting the given overall criteria is obtained when ϵ becomes less than or equal to δ_p.

Appendix B

This appendix shows how to properly optimize $G_1(z)$, $G_2(z)$, and $G_3(z)$ at Step 3 of the algorithm of Sec. 5 in a manner similar to that used for optimizing $G_1(z)$ and $G_2(z)$ at Step 2 of the algorithm described in Sec. 3.1.

There exist the following two cases under consideration. In the first case, $G_2(z)$ is of even order N_2 and $G_1(z) = z^{-N_2/2}$, whereas in the second case, $G_1(z)$ is of even order N_1 and $G_2(z) = z^{-N_1/2}$. In both cases, N_3, the order of $G_3(z)$, can be either even or odd. In the first case, the problem is to find the impulse-response values of $g_2(n)$ for $n = 0, 1, \ldots, (N_2/2)$ and $g_3(n)$ for $n = 0, 1, \ldots, \lfloor N_3/2 \rfloor$ to minimize $\epsilon_G^{(r)}$, as given by Eq. (7a), where now

$$H_G^{(r)}(\omega) = F^{(r-1)}(L\omega) G_3^{(r)}(\omega) + \left[1 - F^{(r-1)}(L\omega)\right] G_2^{(r)}(\omega) G_3^{(r)}(\omega)\,, \tag{B.1}$$

whereas, in the second case, the adjustable parameters are $g_1(n)$ for $n = 0, 1, \ldots, (N_1/2)$ and $g_3(n)$ for $n = 0, 1, \ldots, \lfloor N_3/2 \rfloor$ and

$$H_G^{(r)}(\omega) = F^{(r-1)}(L\omega) G_1^{(r)}(\omega) G_3^{(r)}(\omega) + \left[1 - F^{(r-1)}(L\omega)\right] G_3^{(r)}(\omega)\,. \tag{B.2}$$

These problems are not linear with respect to the unknowns as the problem at Step 2 in Sec. 3.1. Therefore, linear programming cannot be utilized. However, they are solvable by using an unconstrained nonlinear optimization algorithm in a manner similar to that described in Appendix A.

At Step 3 of the algorithm of Sec. 5, the start-up solutions for $F(z^L)$ as well as $G_1(z)$ and $G_3(z)$ [$G_2(z)$ and $G_3(z)$] are directly determined for $G_1(z) = z^{-N_2/2}$ [$G_2(z) = z^{-N_1/2}$], but not for $G_2(z)$ [$G_1(z)$]. It has been observed that the convergence of the algorithm is not very sensitive to the initial solution for the remaining transfer function. Therefore, for $G_1(z) = z^{-N_2/2}$, a good enough starting-point filter is obtained by selecting $g_2(n) = 0$ for $n = 0, 1, \ldots, (N_2/2)$ and for $G_2(z) = z^{-N_1/2}$, by selecting $g_1(n) = 0$ for $n = 0, 1, \ldots, (N_1/2)$.

Appendix C

Tables C.1–C.3 and C.4–C.6 in this appendix give the optimized impulse-response values for the best proposed FRM filter with separate masking filters for $L = 21$ and $\sum_{n=0}^{N_F} f(n) = 1.2$ as well as for the corresponding FRM filter with a common part for the masking filters, respectively.

Table C.1. Impulse-response values of the periodic filter $F(z)$ for the best proposed filter with separate masking filters ($f(122 - n) = f(n)$ for $n = 0, 1, \ldots, 61$).

$f(0) = 0.000361950733324$	$f(21) = 0.001538737458912$	$f(42) = -0.001355056952740$
$f(1) = 0.001435917998936$	$f(22) = 0.001553656805363$	$f(43) = -0.007335254711548$
$f(2) = 0.001630124957917$	$f(23) = -0.000848790217131$	$f(44) = -0.002436765909279$
$f(3) = 0.001139699493582$	$f(24) = -0.002207798494002$	$f(45) = 0.007201300939444$
$f(4) = 0.000003301348073$	$f(25) = -0.000216406040542$	$f(46) = 0.006832840674540$
$f(5) = -0.000327716340805$	$f(26) = 0.002395406292746$	$f(47) = -0.004602956707566$
$f(6) = 0.000289761357718$	$f(27) = 0.001591793369477$	$f(48) = -0.010570153283156$
$f(7) = 0.000887708979211$	$f(28) = -0.001814468256261$	$f(49) = -0.000340635317258$
$f(8) = 0.000373155547312$	$f(29) = -0.002759639723909$	$f(50) = 0.012607510230171$
$f(9) = -0.000568102925605$	$f(30) = 0.000557163596824$	$f(51) = 0.007587230939461$
$f(10) = -0.000620519658457$	$f(31) = 0.003446214195436$	$f(52) = -0.011221322026826$
$f(11) = 0.000484695704472$	$f(32) = 0.001271564186322$	$f(53) = -0.015903685792009$
$f(12) = 0.001044071098951$	$f(33) = -0.003165770485932$	$f(54) = 0.005465337293915$
$f(13) = 0.000155790703074$	$f(34) = -0.003143648101756$	$f(55) = 0.024737746204905$
$f(14) = -0.001072670890515$	$f(35) = 0.001890628024176$	$f(56) = 0.007416167910198$
$f(15) = -0.000682995743820$	$f(36) = 0.004604447739654$	$f(57) = -0.031567899775798$
$f(16) = 0.000885197454628$	$f(37) = 0.000399785630749$	$f(58) = -0.031992041519941$
$f(17) = 0.001340158672739$	$f(38) = -0.004976843383474$	$f(59) = 0.038019760324954$
$f(18) = -0.000229565706170$	$f(39) = -0.003139192110345$	$f(60) = 0.103779719239076$
$f(19) = -0.001607198344393$	$f(40) = 0.003972345045533$	$f(61) = 0.985602439035551$
$f(20) = -0.000597323026857$	$f(41) = 0.005782983103399$	

Table C.2. Impulse-response values of the masking filter $G_1(z)$ for the best proposed filter with separate masking filters ($g_1(55-n) = g_1(n)$ for $n = 0, 1, \ldots, 27$).

$g_1(0) = 0.002340220275119$	$g_1(10) = 0.001934323808919$	$g_1(20) = -0.002601145500567$
$g_1(1) = 0.003503021007655$	$g_1(11) = 0.012601586444752$	$g_1(21) = 0.041008369697269$
$g_1(2) = 0.002420810217345$	$g_1(12) = 0.010371183081417$	$g_1(22) = 0.033098912977289$
$g_1(3) = -0.000960389367473$	$g_1(13) = -0.005498330279802$	$g_1(23) = -0.039172776560799$
$g_1(4) = -0.002859510670150$	$g_1(14) = -0.015427197995161$	$g_1(24) = -0.086749791832917$
$g_1(5) = 0.000023050145394$	$g_1(15) = -0.001231439898475$	$g_1(25) = -0.003874457401399$
$g_1(6) = 0.003777158245435$	$g_1(16) = 0.019560247502404$	$g_1(26) = 0.199821729315399$
$g_1(7) = 0.002915014946574$	$g_1(17) = 0.015882520553606$	$g_1(27) = 0.377218739612221$
$g_1(8) = -0.003033911278315$	$g_1(18) = -0.014796173164523$	
$g_1(9) = -0.006356958291979$	$g_1(19) = -0.031908494913373$	

Table C.3. Impulse-response values of the masking filter $G_2(z)$ for the best proposed filter with separate masking filters ($g_2(77-n) = g_2(n)$ for $n = 0, 1, \ldots, 38$).

$g_2(0) = 0.012965493580397$	$g_2(13) = -0.022358781524541$	$g_2(26) = 0.070546046881574$
$g_2(1) = 0.023420938922838$	$g_2(14) = -0.046512327439832$	$g_2(27) = 0.055694400894129$
$g_2(2) = 0.017821613847169$	$g_2(15) = -0.010960135430211$	$g_2(28) = -0.040421303974270$
$g_2(3) = -0.002453752677662$	$g_2(16) = 0.041666666607170$	$g_2(29) = -0.086693745171066$
$g_2(4) = -0.017954267081655$	$g_2(17) = 0.039342721073975$	$g_2(30) = -0.011756915811254$
$g_2(5) = -0.003512516770742$	$g_2(18) = -0.020209438574448$	$g_2(31) = 0.087480253396182$
$g_2(6) = 0.018637771637562$	$g_2(19) = -0.056295991221633$	$g_2(32) = 0.089639192405058$
$g_2(7) = 0.017720662241110$	$g_2(20) = -0.013746677273513$	$g_2(33) = -0.020381258875616$
$g_2(8) = -0.010985399233433$	$g_2(21) = 0.046663487252768$	$g_2(34) = -0.100178215159426$
$g_2(9) = -0.029550409545783$	$g_2(22) = 0.033824754523678$	$g_2(35) = -0.047047654303128$
$g_2(10) = -0.006712872218914$	$g_2(23) = -0.040672115471946$	$g_2(36) = 0.098893308096891$
$g_2(11) = 0.025810121946954$	$g_2(24) = -0.074609199328606$	$g_2(37) = 0.235060004209916$
$g_2(12) = 0.021786016577949$	$g_2(25) = -0.007892093581375$	$g_2(38) = 0.294705919407159$

Table C.4. Impulse-response values of the periodic filter $F(z)$ for the best proposed filter with a common part for the masking filters ($f(122-n) = f(n)$ for $n = 0, 1, \ldots, 61$).

$f(0) = 0.003646457237418$	$f(21) = 0.013197212992604$	$f(42) = -0.011834623247256$
$f(1) = 0.012783627099498$	$f(22) = 0.013159553633415$	$f(43) = -0.062045275200354$
$f(2) = 0.014863495329740$	$f(23) = -0.007164751228535$	$f(44) = -0.020123353906613$
$f(3) = 0.010529390730637$	$f(24) = -0.018587591732305$	$f(45) = 0.061228137676814$
$f(4) = 0.000799875890405$	$f(25) = -0.001627199396164$	$f(46) = 0.057357137903337$
$f(5) = -0.002266545618958$	$f(26) = 0.020407495556029$	$f(47) = -0.039448170904538$
$f(6) = 0.002803502017934$	$f(27) = 0.013420490048974$	$f(48) = -0.089098084791278$
$f(7) = 0.007752451696323$	$f(28) = -0.015370251504229$	$f(49) = -0.001796643617391$
$f(8) = 0.003246336618119$	$f(29) = -0.023244672432363$	$f(50) = 0.107020780941783$
$f(9) = -0.004662500284521$	$f(30) = 0.004932690757409$	$f(51) = 0.063117814042555$
$f(10) = -0.005159622536667$	$f(31) = 0.029211163038778$	$f(52) = -0.095713677028632$
$f(11) = 0.004270661016163$	$f(32) = 0.010611012355543$	$f(53) = -0.133049074068012$
$f(12) = 0.008892603736253$	$f(33) = -0.026847328283664$	$f(54) = 0.049223808985837$
$f(13) = 0.001335536081315$	$f(34) = -0.026463123518720$	$f(55) = 0.209329314062799$
$f(14) = -0.009019511759854$	$f(35) = 0.016219429013750$	$f(56) = 0.058580427662827$
$f(15) = -0.005675152316453$	$f(36) = 0.038887376475652$	$f(57) = -0.268200360253062$
$f(16) = 0.007651758031989$	$f(37) = 0.003122040361711$	$f(58) = -0.256653235721140$
$f(17) = 0.011382986867556$	$f(38) = -0.042179653743201$	$f(59) = 0.345654680767036$
$f(18) = -0.001926844002531$	$f(39) = -0.026322356339269$	$f(60) = 0.869968988342555$
$f(19) = -0.013520673582904$	$f(40) = 0.033855240989724$	$f(61) = 0.876453641366017$
$f(20) = -0.004897685117621$	$f(41) = 0.048707663490742$	

Table C.5. Impulse-response values of the masking filter $G_2(z)$ for the best proposed filter with a common part for the masking filters ($g_2(46-n) = g_2(n)$ for $n = 0, 1, \ldots, 23$).

$g_2(0) = 0.076322909107322$	$g_2(8) = -0.071322828158018$	$g_2(16) = 0.098531511393780$
$g_2(1) = -0.206934343494090$	$g_2(9) = -0.052306754652771$	$g_2(17) = 0.015926958782351$
$g_2(2) = 0.205463762032903$	$g_2(10) = 0.128526603491643$	$g_2(18) = -0.062963276302559$
$g_2(3) = -0.020297534439983$	$g_2(11) = -0.049102289317657$	$g_2(19) = -0.052554910937778$
$g_2(4) = -0.083989582846649$	$g_2(12) = -0.049838805662072$	$g_2(20) = 0.091578819747781$
$g_2(5) = -0.029584108607911$	$g_2(13) = 0.088515609088459$	$g_2(21) = -0.011667396163315$
$g_2(6) = 0.102994638386742$	$g_2(14) = -0.051266486403238$	$g_2(22) = 0.009768822550636$
$g_2(7) = 0.017416979835096$	$g_2(15) = -0.061243094134045$	$g_2(23) = 0.948717560946144$

Table C.6. Impulse-response values of the common masking filter $G_3(z)$ for the best proposed filter with a common part for the masking filters ($g_3(55-n) = g_3(n)$ for $n = 0, 1, \ldots, 27$).

$g_3(0) = 0.000507309554468$	$g_3(10) = -0.001538919107299$	$g_3(20) = -0.003336781960600$
$g_3(1) = 0.002720099724907$	$g_3(11) = 0.008947853775008$	$g_3(21) = 0.042579863250077$
$g_3(2) = 0.001172077206392$	$g_3(12) = 0.008654921515382$	$g_3(22) = 0.036551711506846$
$g_3(3) = -0.001442331493624$	$g_3(13) = -0.006757858924079$	$g_3(23) = -0.034711604820987$
$g_3(4) = -0.004019993920281$	$g_3(14) = -0.015671431180178$	$g_3(24) = -0.084227617066338$
$g_3(5) = -0.000796457544281$	$g_3(15) = -0.002047548400590$	$g_3(25) = -0.003192541056794$
$g_3(6) = 0.004586808435845$	$g_3(16) = 0.019247472816000$	$g_3(26) = 0.199641043278351$
$g_3(7) = 0.004205254789063$	$g_3(17) = 0.016495343289950$	$g_3(27) = 0.376803808522285$
$g_3(8) = -0.003510424292365$	$g_3(18) = -0.013986861849270$	
$g_3(9) = -0.008573397649704$	$g_3(19) = -0.031980282030935$	

References

1. Y. C. Lim, "Frequency-response masking approach for the synthesis of sharp linear phase digital filters", *IEEE Trans. Circuits Syst.* **CAS-33** (1986) 357–364.
2. Y. C. Lim and Y. Lian, "The optimum design of one- and two-dimensional FIR filters using the frequency response masking technique", *IEEE Trans. Circuits Syst. II* **40** (1993) 88–95.
3. T. Saramäki, "Design of computationally efficient FIR filters using periodic subfilters as building blocks", *The Circuits and Filters Handbook*, ed. W.-K. Chen, CRC Press, Inc., 1995, pp. 2578–2601.
4. T. Saramäki and Y. C. Lim, "Use of the Remez algorithm for designing FRM based FIR filters", *Circuits, Systems, and Signal Processing* **22**, 2 (2003) 77–97; T. Saramäki and Y. Lian (eds.), *Special Issue on Frequency Response Masking Technique and Its Applications.*
5. Y. C. Lim and Y. Lian, "Frequency-response masking approach for digital filter design: Complexity reduction via masking filter factorization", *IEEE Trans. Circuits Syst. II* **41** (1994) 518–525.
6. T. Saramäki and H. Johansson, "Optimization of FIR filters using the frequency-response masking approach", *Proc. IEEE Int. Symp. Circuits Syst.*, Sydney, Australia, 2001, pp. 177–180.
7. T. Saramäki and J. Yli-Kaakinen, "Optimization of frequency-response-masking based FIR filters with reduced complexity", *Proc. IEEE Int. Symp. Circuits Syst.*, Scottsdale, Arizona, 2002, pp. 225–228. http://alpha.cc.tut.fi/∼ylikaaki/3135.pdf.

8. J. H. McClellan, T. W. Parks, and L. R. Rabiner, "A computer program for designing optimum FIR linear phase digital filters", *IEEE Trans. Audio Electroacoust.* **AU-21** (1973) 506–526. Also reprinted in *Selected Papers in Digital Signal Processing, Vol. II*, edited by the Digital Signal Processing Commitee and IEEE ASSP Society, IEEE Press, New York, 1975, pp. 97–117.
9. T. Coleman, M. A. Branch, and A. Grace, *Optimization Toolbox User's Guide*, The MathWorks, Inc., Version 2, 1999.

Copyright of Journal of Circuits, Systems & Computers is the property of World Scientific Publishing Company and its content may not be copied or emailed to multiple sites or posted to a listserv without the copyright holder's express written permission. However, users may print, download, or email articles for individual use.